Available online at www.sciencedirect.com
ScienceDirect
International Journal of Fatigue 29 (2007) 254–260
International Journal of Fatigue
www.elsevier.com/locate/ijfatigue

Fatigue crack growth retardation in an HSLA steel in benign environments

A. Roy [a], S. Tarafder [a], S. Sivaprasad [a], Swapan K. Das [a], I. Manna [b], I. Chattoraj [a,*]

[a] National Metallurgical Laboratory, Jamshedpur 831 007, India
[b] Indian Institute of Technology, Kharagpur 721 302, India

Received 23 December 2005; received in revised form 9 March 2006; accepted 17 March 2006
Available online 5 May 2006

Abstract

The crack growth and closure were examined for fatigue loading of an HSLA steel in non-corroding media. R and ΔK dependent significant crack growth retardation was observed in NaOH. Presence of a passive film at high R and self repair of the film and formation of an additional oxide layer at low R could explain the retardation.

Keywords: Crack closure; Crack growth rate; Stress ratio (R); Steel; Passive film

1. Introduction

Fatigue crack growth of different grades of steels have been extensively reported in different environments [1–17]. For the most part, these environments, liquid or gaseous [4,7,11–16], were chosen to be intentionally deleterious, providing crack growth enhancement. In studies on environments, the environmental issues of importance to crack growth are anodic dissolution [1], crack closure [6,7], adsorption of deleterious species [11,13,14] and hydrogen (H) enhanced cracking or H embrittlement [2–5,8–10,12,13,15]. In instances where the environment had produced crack growth retardation [6], it was mostly due to crack closure by oxide film or corrosion product accumulated on the crack face. There is little or no literature on fatigue testing of steels in non-corroding or benign aqueous environments, or in sustained passivating environments. And correspondingly there is not a proper understanding of the role of sustained passive films on crack growth in steels.

This work studies crack growth in a few systems where there is no corrodent and therefore and otherwise, the H effects are low. The major emphasis of this work was on investigating crack growth in a spontaneously passivating media (where even the new crack faces formed on crack propagation get passivated quickly) and to highlight the role of passive film in crack propagation.

2. Experimental

The material used in this study was a Cu strengthened HSLA steel with a chemical composition [in wt%: C – 0.05, Mn – 1.00, P – 0.009, S – 0.001, N – 0.01, Si – 0.34, Cr – 0.61, Mo – 0.51, Al – 0.025, Nb – 0.037, Ni – 1.77, Cu – 1.23, Fe – balance]. It was obtained in the form of rolled plates 2'' (50 mm) thick. The steel had an acicular ferrite microstructure, a tensile strength of 740 MPa, an uniaxial yield strength (σ_{ys}) of 650 MPa, and a hardness of 280 VPN. Fatigue tests were conducted using notched three point bend (TPB) specimens with nominal dimensions of $100 \times 20 \times 10$ mm. Prior to fatigue tests, all specimens were pre cracked up to 2 mm in air. Suitable precautions were taken to avoid overload effects. The fatigue tests were conducted at room temperature using the

* Corresponding author.
E-mail address: ichatt_62@yahoo.com (I. Chattoraj).

0142-1123/$ - see front matter
doi:10.1016/j.ijfatigue.2006.03.010

procedure laid down in ASTM standard E 647. The tests were conducted in the ΔK regime of 28 to 15 MPa $m^{0.5}$ which fell within the Stage II crack growth regime for this steel in air. The fatigue crack growth rate (FCGR) tests were conducted with a decreasing ΔK protocol with constant R ($= K_{min}/K_{max}$) at a frequency of 1 Hz. The compliance crack length relation was used for the on-line crack length measurements using a 5 mm COD gauge. Crack closure was monitored based on the procedure laid down in ASTM standard E 647. Fatigue crack growth rates (da/dN) were computed on-line by the 7-point incremental polynomial method. The experiments were duplicated or triplicated to gain confidence with the results. The most representative crack growth curves are presented.

Tests in the different aqueous environments were conducted in a stainless steel tank attached to the lower ram of the loading frame. All tests were conducted open to atmosphere. The two aqueous environments used were distilled water and 0.1 N NaOH. The fatigue tests were continued till predefined crack length levels. After completion of the fatigue tests, the samples were broken open by overload, and cleaned with running water and then acetone (for samples tested in air, only acetone was used). The fracture surfaces were observed under a scanning electron microscope (SEM). The crack length was normally large enough to differentiate between the crack surface produced in the high ΔK regime and that produced in the low ΔK regime. The observations were recorded so as to demarcate the different ΔK regimes of the fracture surface. The corrosion product remnant on the fracture surface was subjected to elemental analysis by energy dispersive spectroscopy (EDS).

3. Results

3.1. Crack growth and closure

The da/dN vs ΔK plot and da/dN vs ΔK_{eff} plot of HSLA-80 steels at $R = 0.1$ and at 1 Hz frequency in different environments are shown in Figs. 1 and 2, respectively. The crack growth rate was found to be higher in water as compared with that in air and in the 0.1 N NaOH solution when plotted without compensating for crack closure. The crack growth rate in the NaOH solution was initially (at high ΔK) close to the values for air. But at intermediate and low ΔK values, it was significantly lower than the crack growth rate in air. The plot of da/dN vs ΔK_{eff}, shown in Fig. 2, demonstrates the closure effect. Similar crack growth rates, after closure compensation, were observed in the high ΔK region for all the environments. However, in the lower ΔK region, crack growth rate was found to be higher in water than in air. This could probably be due to low but finite H availability from the corrosion reactions in water. It was also reflective of the ineffectiveness of the corrosion product formed in water in bringing about crack closure. Even after closure compensation, the crack growth rate in the 0.1 N NaOH was significantly less than

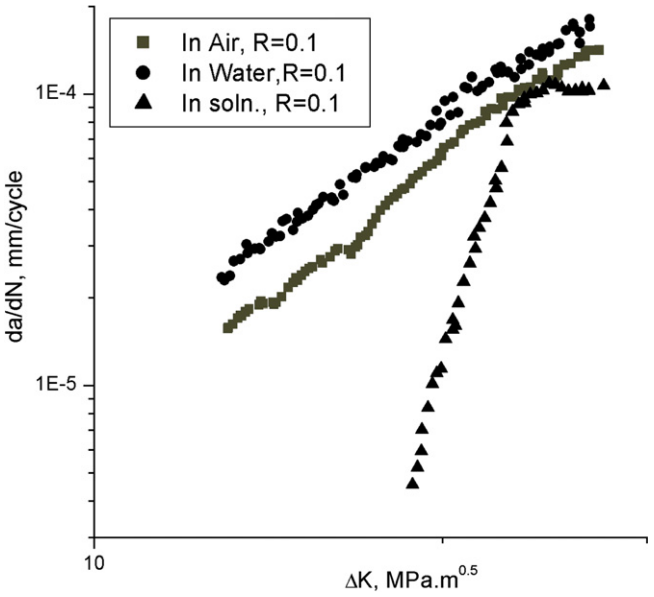

Fig. 1. Crack growth in different environments.

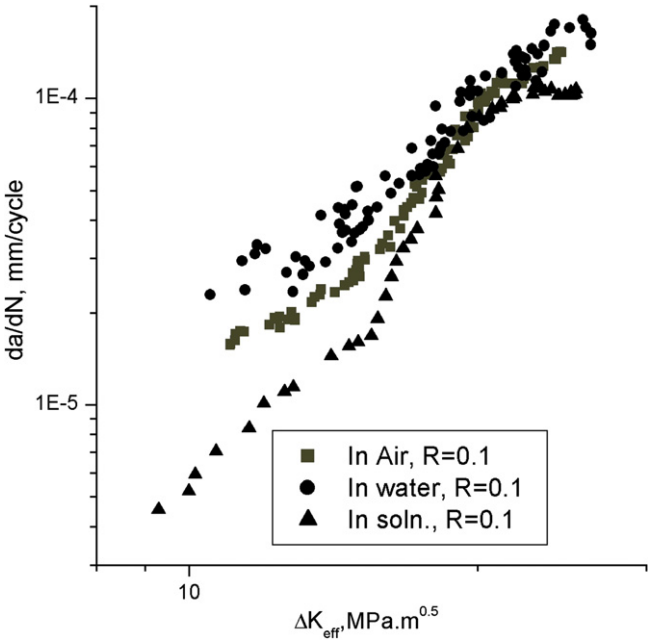

Fig. 2. Crack growth in different environments after closure compensation.

that in air, clearly indicating that crack retardation was due to effects above and beyond closure effects. A better idea of the closure extent can be obtained from a plot of K_{cl}/K_{max} vs ΔK in the different environments (Fig. 3), where K_{cl} is the K on crack closing in any given load cycle. The K_{cl}/K_{max} increases up to 0.5 with decreasing ΔK for test in the NaOH solution. Closure was observed in all the three environments, as is apparent from K_{cl}/K_{max} value consistently being greater than the R. The K_{cl}/K_{max} values were slightly higher in air than in water.

To further explore the unaccounted crack retardation in the NaOH solution, FCGR tests were conducted in the

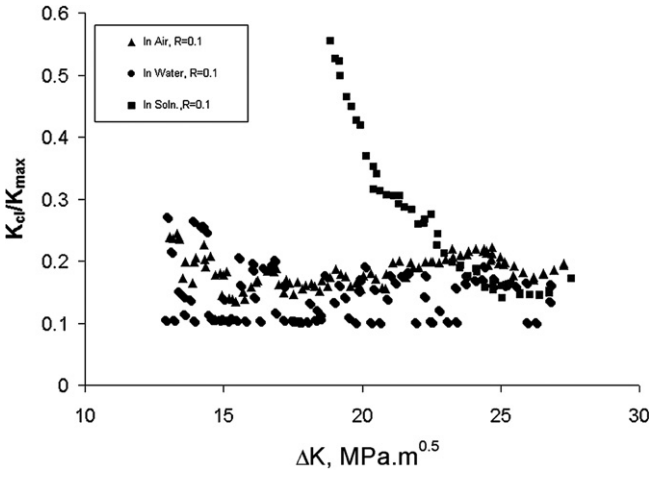

Fig. 3. Extent of crack closure in different environments for $R = 0.1$. A positive deviation of K_{cl}/K_{max} from R (=0.1) indicates closure.

solution with different R ratios. The results for the crack growth at different R ratios, as a function of ΔK are shown in Fig. 4 and as a function of ΔK_{eff} in Fig. 5. The data for crack growth in air are also included for comparison; it needs to be stated here that the crack growth rate in air was very similar for different R ratios. There are several interesting observations evident from Figs. 4 and 5. The crack growth rate is lower than that in air for almost the entire ΔK regime when the fatigue tests were conducted at the higher R ratios (0.3 and 0.5), however for both these R values the crack growth rate merges with that for air at low ΔK values. In contrast, at the lower R values of 0.1 and 0.2, the crack growth rates start off lower than that for air. For certain intermediate ΔK values, it merges with that for air, and subsequently drops off below the crack growth line

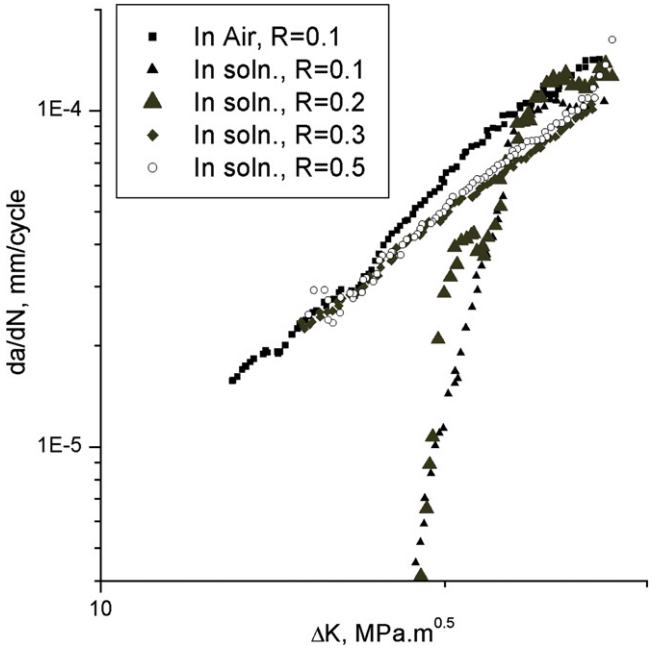

Fig. 4. Crack growth in 0.1 N NaOH for different R ratios.

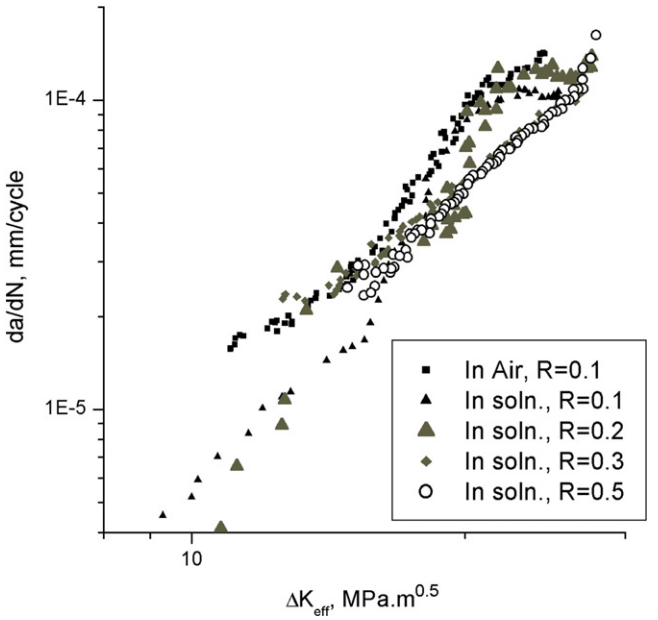

Fig. 5. Crack growth in 0.1 N NaOH for different R ratios after closure compensation.

for air. Most interestingly, at low ΔK values, the crack growth rates are significantly lower than that for air as well as for the higher R values in solution. From Fig. 5, it is evident that part of this crack retardation can be attributed to closure, but even after closure compensation, the crack growth rates still show significantly lower values than that for air. For samples tested in solution at higher R values (0.3 and 0.5), there is no or insignificant closure. This can be appreciated better from a comparison of the K_{cl}/K_{max} normalised by R, with crack progression, as shown in Fig. 6 for the different R ratios. For $R = 0.5$ this ratio stays at 1 for the entire crack growth regime indicating no

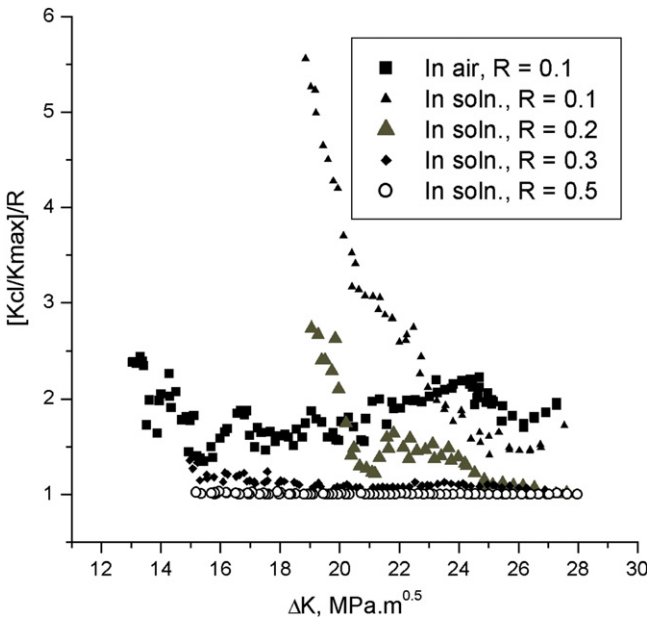

Fig. 6. Extent of crack closure in 0.1 N NaOH for different R ratios.

closure at all ΔK values; for $R = 0.3$, there is insignificant closure. There is significant closure effect in the cases of low R tests (Fig. 6), this effect increasing as the crack progresses, that is with decreasing ΔK. The intriguing observation is that closure cannot account completely for the crack growth retardation at any of the R values when tested in NaOH: there is no closure at high Rs and retardation above and beyond that produced by closure for low Rs. Although the crack growth in NaOH at the low R values (0.1 and 0.2) are quite similar, there are observable differences too. The closure is much more pronounced in $R = 0.1$ (Fig. 6); additionally the tests at $R = 0.2$ show a region corresponding to intermediate ΔK_{eff} where the crack growth is very similar to that for air and the higher R tests in solution, once closure is discounted. Subsequently (that is, at lower ΔK and ΔK_{eff}) the crack growth rate for $R = 0.2$ approaches and merges with that for $R = 0.1$.

3.2. Fractography

Samples fatigue tested in air showed normal fibrous fracture surface (Fig. 7) with little difference in the high ΔK (Fig. 7(a)) and low ΔK regions (Fig. 7(b)) of the fracture surface. In the sample exposed to water, there was evidence of corrosion and general degradation of the surface (Fig. 8). This was in the form of local areas of metal dissolution and corrosion product deposition (indicated by circle in Fig. 8). There were very small granular deposits and the crack surface features were less delineated as compared to Fig. 7. However the remnant corrosion product on the fracture surface was insignificant. The fracture surface corresponding to the high and low ΔK regions are shown for the sample tested in the 0.1 N NaOH solution at $R = 0.1$ in Fig. 9. The high ΔK features (Fig. 9(a)) are very similar to that for tests in air (Fig. 7). In the low ΔK region, a thick and adherent reaction product layer was observed (Fig. 9(b)) which was thick enough to prevent observation of the underlying metal surface. A lower magnification photograph of the fracture surface clearly shows the delineation of the two regions (Fig. 10). The observable adherent layer was found to be oxygen rich by EDS as shown in Fig. 11. The line profile of the line indicated in Fig. 10(a) also showed a variation in the oxygen content across the fracture surface (Fig. 10(b)). It was evident that for $R = 0.1$, except for the initial stages (high ΔK) of crack growth, an adherent oxygen rich film developed on the crack faces. The fracture surface for the sample tested in the 0.1 N NaOH solution at $R = 0.5$ and $R = 0.3$ showed no oxide film on the crack surface corroborating the lack of closure observed. The fractographic observations for

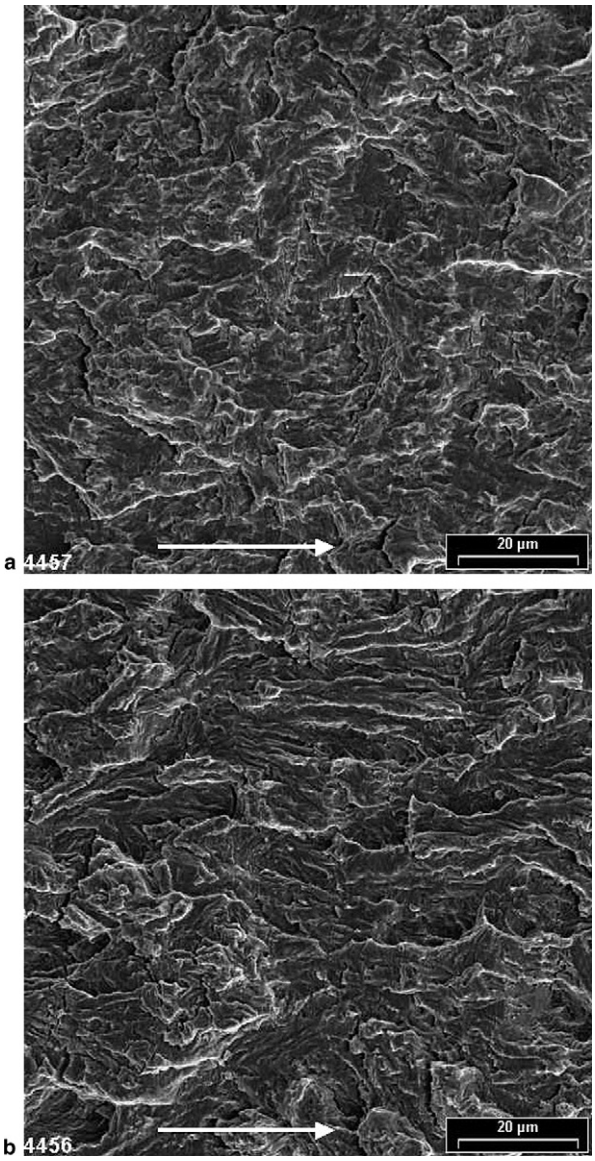

Fig. 7. Fracture surface of sample tested in air at $R = 0.1$ and 1 Hz corresponding to high ΔK regime (a); and corresponding to low ΔK regime (b). The white arrow indicates the direction of crack growth.

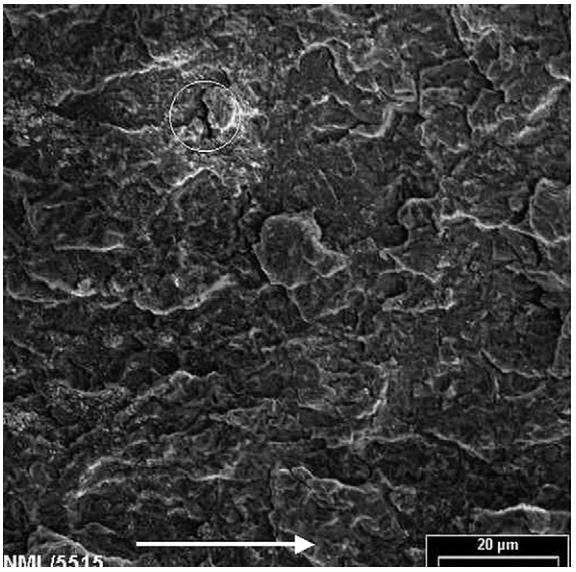

Fig. 8. Fracture surface of sample tested in distilled water at $R = 0.1$ and 1 Hz. Metal loss and some corrosion debris are observed. The white arrow indicates the direction of crack growth.

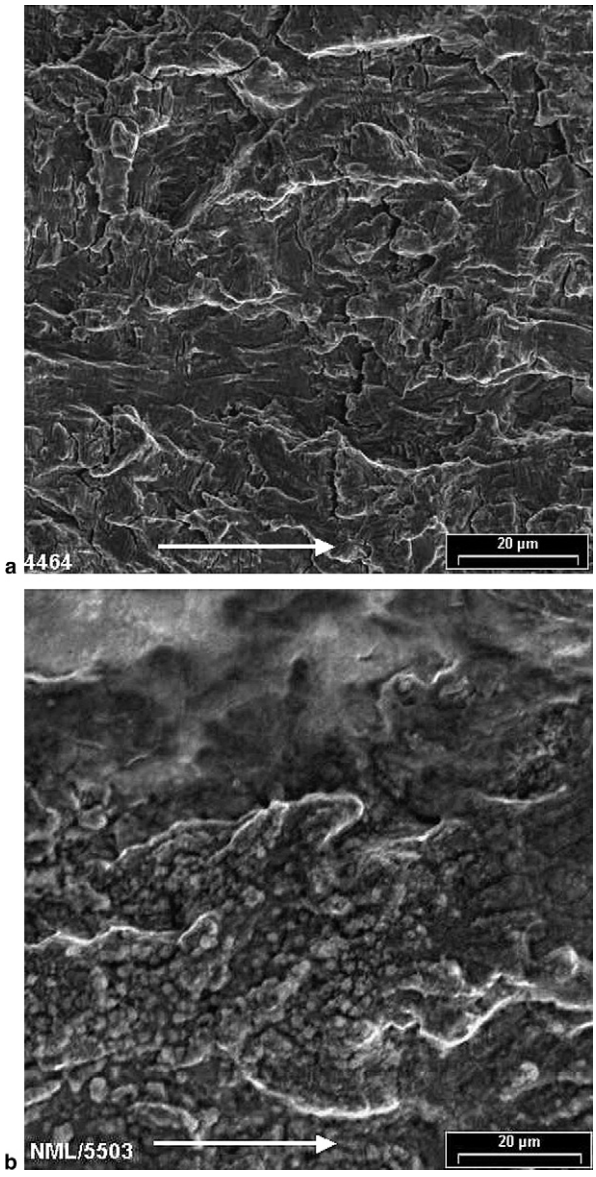

Fig. 9. Fracture surface of sample tested in 0.1 N NaOH at $R = 0.1$ and 1 Hz corresponding to high ΔK regime (a); and corresponding to low ΔK regime (b). The latter shows a thick, adherent, oxygen rich layer on the crack surface. The white arrow indicates the direction of crack growth.

$R = 0.2$ (Fig. 12) also showed a thick oxide film in the intermediate ΔK regimes akin to $R = 0.1$ samples (similar to Fig. 9(b)) but there were regions on the crack surface that were devoid of the oxygen rich layer. The oxygen profile across the crack face as shown in Fig. 12(b) corroborates this lack of oxygen rich layer close to the crack tip. The region of the crack face devoid of the layer corresponds approximately to the part of the crack face that was produced at ΔK_{eff} values when the crack growth approached that for air.

4. Discussion

The results of the fatigue tests conducted in the different environments show some similarities and certain differences. For fatigue tests in air, there was some closure effect observed. The crack growth rates may be reduced by oxide-induced closure, although such oxide layers are not

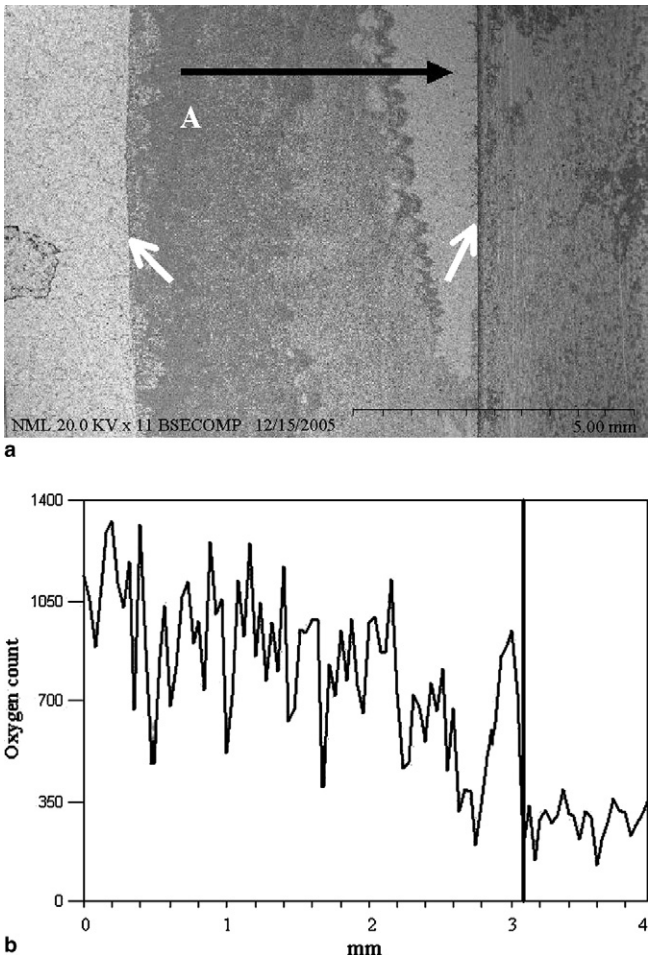

Fig. 10. Low magnification photograph of the fracture surface of sample tested in 0.1 N NaOH at $R = 0.1$ and 1 Hz; the white arrows on the right and left indicate the precracked region and the overload rupture fractures, respectively (a); the oxygen concentration variation along the line indicated in (a), the black marker separates the region with and without a reaction layer (b).

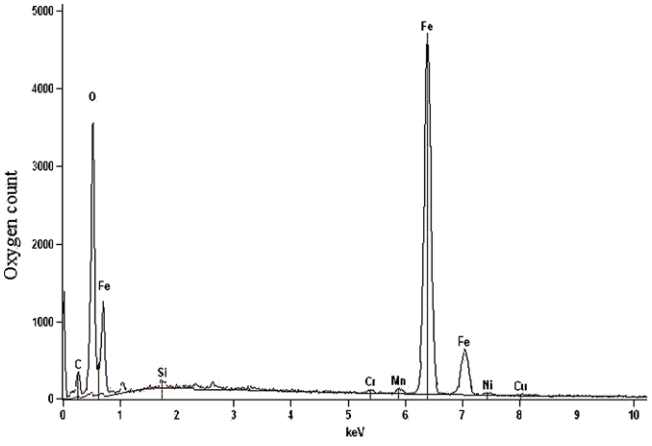

Fig. 11. Energy dispersive spectroscopic analysis of the thick adherent layer shown in Fig. 10 (a) at the point marked "A". Oxygen is observed as a significant element.

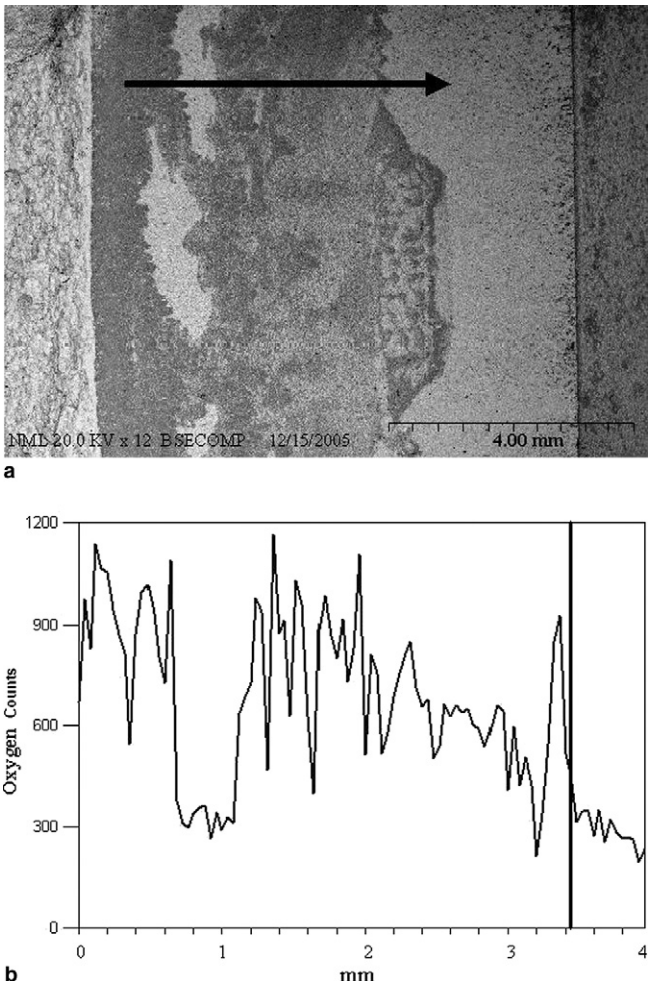

Fig. 12. Low magnification photograph of the fracture surface of sample tested in 0.1 N NaOH at $R = 0.2$ and 1 Hz, certain regions on the fracture surface are devoid of the reaction layer (a); the oxygen concentration variation along the line indicated in (a), the oxygen absence in the regions devoid of the reaction layer is evident (b).

resolvable on the fracture surface. Crack growth rate was found to be higher in water as compared to air, which can be attributed to anodic dissolution and hydrogen enhanced crack growth. This is similar to the reported findings [9,14] which showed higher crack growth in pure or distilled water compared to air. The closure was the least in water as compared to the other environments tested in this study, which is also borne out by the absence of any significant oxide film or corrosion product suggesting an inability of the metal to develop adherent oxide film in pure water.

The crack growth rate in NaOH is markedly influenced by the R value. A passive film spontaneously forms on the steel surface in 0.1 N NaOH, which was borne out by electrochemical polarization tests. This is reported to be magnetite along with γ-FeOOH [17], however it was beyond the scope of this investigation to chemically or otherwise characterise this film. Our explanation of the behavior in NaOH is based on the presence, breakdown and transformation of this passive layer. Tests at high R values meant that the crack face separation was large enough for almost the entire ΔK range, so that the passive film was not compromised by crack face rubbing. Only near the end of the tests (low ΔK regime), this passive film would have been removed by crack face contact, and the crack growth rates approached that in air. Needless to say, the passive film, which is normally very thin, does not provide closure effects. For low R tests, the passive film was compromised even at high ΔK, so that the crack growth approached that in air very soon after initiation of the test. What emerges from the SEM observation is that another thick, possibly oxide, film developed as the cracking progressed, which was adherent to the surface. This thick adherent oxygen rich film was consistently found in the lower ΔK regimes for the low R tests in NaOH. The necessity for the breakdown of the passive film to create the overlying oxygen rich film is brought out by the sporadic absence of such a film in the $R = 0.2$ tests when the crack face rubbing is less severe than for $R = 0.1$. We propose that in addition to this transformation, the passive film repaired itself with time (the overlying porous film allows easy access of the solution to the metal substrate) so that at low ΔK values and low R ratios, the metal had a thin film of passive layer under a thick observable oxide layer. The formation of the adherent overlying film caused closure and crack growth retardation for tests at low Rs, and the closure increased as crack progressed (lower ΔKs). In addition, this overlying thick layer protected the underlying passive film during crack face contact, thereby extracting the benefits of the passive layer on crack growth retardation. The passive films formed on steels in NaOH are a few atomic layers thick and could not be separately resolved. However, its presence is indicated in the decrease in crack growth above and beyond that due to closure as observed in Fig. 5. Therefore at low ΔK, for the low R tests, the dual benefits of closure and passive film protection, lead to crack growth retardation much greater than that observed for high R tests at similar ΔK values.

The possible protection mechanism of the passive film is discussed in the following. There is no literature on the role of a true passive film on fatigue crack growth. When passivating alloys, like stainless steels, have been studied, the emphasis has been to provide environments that promote passive film breakdown like chloride or concentrated alkali media, with no scope for spontaneous repair. In this regard studies comparing crack growths in vacuum vis-à-vis air and other environments [11–15] are instructive. The recurring findings in those works was that crack growth rates were lower in vacuum due to the absence of adsorption of extraneous species like H or O. The crack growth enhancement in environments including air is attributed to a decrease in the crack surface energy by adsorption, to H embrittlement effects or to the interaction of the adsorbed species with localised slip and dislocation multiplication. It has also been reported that certain gaseous species like CO can retard crack growth by preferentially adsorbing on crack surfaces nullifying the embrittling effect of H [15]. We feel, that the passive film, especially a spontaneous passive film as would form in NaOH on steel,

would prevent the adsorption of such deleterious species, thereby providing crack growth retardation. Passivation is instantaneous on newly formed crack surfaces, preventing such adsorption. Therefore, in NaOH, the crack retardation at all R ratios occurred due to the presence of a passive film, over and above crack retardation due to closure, the latter being observed only at low R ratios (due to the thick oxide film). The difference in the protection provided by the passive layer for the tests carried out at high Rs and low Rs, is due to the fact that in the latter, the exclusion of deleterious species is brought about by a dual film – a oxide rich observable layer and the underlying passive film. This is borne out by the fact that when the samples tested at $R = 0.2$ were devoid of the overlying film, the crack growth rate was same as for that in high Rs.

5. Conclusions

The fatigue crack growth of an HSLA steel in a few non-corroding systems have been studied. Crack growth in water was found to be higher than that in air due to anodic dissolution and possible H embrittlement effects, and minimum crack closure was observed due to absence of adherent corrosion product or oxide film. In NaOH solution the crack growth was significantly less than that in air and this effect was R and ΔK dependent. At high Rs, this could be attributed to the formation of a passive film which is not compromised by crack face contact as the crack face separation are significant at high R for almost all ΔK values. On the other hand at low Rs, the passive film undergoes repeated breakdown and repair and an additional thick reaction layer is formed which subsequently provides closure. It is proposed that this overlying film allows repair of the underlying passive film, and additionally protects it from breakdown at low ΔK values. The passive film acts by preventing adsorption of embrittling species like H or O from the media onto the crack tip and crack surface.

Acknowledgment

The first author is grateful to the Council of Scientific and Industrial Research, India, for a fellowship under its JRF-GATE scheme.

References

[1] Lee DN, Lee SK. Corrosion fatigue of SAE 51100 steel in 3% NaCl solution. Mater Sci Technol 1989;5(5):477–86.
[2] James LA. Surface-crack aspect ratio development during corrosion–fatigue crack growth in low-alloy steels. Nucl Eng Design 1997;172 (1–2):61–71.
[3] Hamano R. Fatigue crack growth from stage I to stage II in a corrosive environment. Int J Fatigue 1997;19(Suppl. 1):S197–204.
[4] Marsh PG, Gerberich WW. Influence of microstructure and texture on fatigue crack initiation in HSLA steel in hydrogen and nitrogen atmospheres. In: First international conference on microstructures and mechanical properties of aging materials, Chicago. The Minerals, Metals & Materials Society (TMS); 1993. p. 287–92.
[5] Thomas JP, Wei RP. Corrosion fatigue crack growth of steels in aqueous solutions. II. Modeling the effects of ΔK. Mater Sci Eng A 1992;A159(2):223–9.
[6] Zhang XD, Song YJ. Crack arrest behaviour and a proposed model. Int J Fatigue 1991;13(5):411–6.
[7] Liaw PK, Leax TR, Donald JK. Gaseous-environment fatigue crack propagation behavior of a low-alloy steel. In: Fracture mechanics: perspectives and directions. Twentieth symposium, Bethlehem, USA; 1989, p. 581–604.
[8] Yamaguchi Y, Nonaka H, Yamakawa K. Effect of hydrogen content on threshold stress intensity factor in carbon steel in hydrogen assisted cracking environments. Corrosion 1997;53(2):147–55.
[9] Li M-Q, Wei Z-W, Zhang F-S, Tang J-Q. The corrosion fatigue of medium strength structural steels. Corros Sci 1993;34(9): 1403–10.
[10] Yamaguchi Y, Nakakura M, Nonaka H. Influences of fatigue frequency and hydrogen content on crack propagation in hydrogen embrittlement environment. J Soc Mater Sci 1996;45(11): 1181–5.
[11] Popp W, Kaesche H. Fatigue crack growth of a low alloy steel in various gaseous environments. Steel Res 1990;61(10):490–7.
[12] Manjunatha CM, King JE. Temperature and environmental effects on fatigue crack growth rate behaviour in Ni–Cr–Mo steel. In: Fatigue 93: 5th International conference on fatigue and fatigue thresholds; 1993, p. 853–58.
[13] Henaff G, Petit J, Bouchet B. Environmental influence on the near-threshold fatigue crack propagation behaviour of a high-strength steel. Int J Fatigue 1992;14(4):211–8.
[14] Tanaka M. The influence of aqueous environments on low ΔK and high ΔK fatigue crack propagation behavior in low carbon structural steels. Metall Mater, Trans A 1996;27A(9):2678–85.
[15] Cotterill PJ, King JE. The influence of a coal gasifier atmosphere on fatigue crack growth rates in BS 43670 steel. Int J Fatigue 1993;15(1):27–30.
[16] Huneau B, Mendez J. Mater Sci Eng A 2003;A345:14.
[17] Joiret S, Keddam M, Novoa XR, Perez MC, Rangel C, Takenouti H. Cement Concrete Compos 2002;24:7.